

Dynamics of elastically strained islands in presence of an anisotropic surface energy

Guido Schifani,^{1,*} Médéric Argentina,¹ and Thomas Frisch¹

¹*Université Côte d'Azur, CNRS, INPHYNI, Nice, France*

Abstract

The equilibrium solutions and coarsening dynamics of strained semi-conductor islands are investigated analytically and numerically. We develop an analytical model to study the effect of surface energy anisotropy on the dynamics coarsening of islands. We propose a simple model to explain the effect of this anisotropy on the coarsening time. We find that the anisotropy slows down the coarsening. This effect is rationalised using a quasi-analytical description of the island profile.

arXiv:1709.08570v1 [cond-mat.soft] 25 Sep 2017

*Electronic address: guido.schifani@inphyni.cnrs.fr

I. INTRODUCTION

The study of elastically strained semi-conductor thin films displays a lot of challenges both from a theoretical and applied point of view [1–3]. The observations of the self-organized strained islands, which arise on these semi-conductor films, has attracted a lot of interest due to their opto-electronic properties for light emitting diode and quantum dots laser [4–6]. In addition, the development of a model that explains the shape and the dynamics of strained islands (quantum dots) remains a fascinating challenge since it involves the dynamical interplay of elastic, capillary, wetting and alloying effects[7–15]. During the deposition or the annealing of the semiconductor film in heteroepitaxy on a substrate, the atomic lattice difference between the film and the substrate induces an elastic stress which can lead to a morphological instability [11, 16–24]. This instability, known as the Asaro-Tiller-Grinfeld (ATG)[25, 26] instability, leads to the formation of parabolic-shaped islands (prepyramid) [27], which have been observed in the nucleation less regime [20, 21]. The prepyramids later evolve in pyramids as more volume is deposited [27]. Later on, the self-organized strained islands displays a coarsening dynamic for which it has been shown theoretically that the surface energy anisotropy slows down the coarsening [28, 29]. The cause of the slowing down of the coarsening can be attributed to several effects is still under investigation and is addressed in this article [10, 28–30].

In this present work, we raise the following question: what is the effect of the amplitude of the surface energy anisotropy on the dynamics of coarsening. We show, using a one-dimensional continuum model and a set of numerical simulations, that coarsening is slowed down as the amplitude of the anisotropy of surface energy increases. Furthermore, we develop a simple model to quantify the effect of the anisotropy of surface energy on the coarsening time. We propose that the main cause of the slowing down of the coarsening is due to the effect of the anisotropy of surface energy. The main effect of the anisotropy of surface energy is to favorize a specific orientation of the surface. This leads to an influence on the shape of the island and thus this affect the distribution of the elastic field in the island. As we shall show, this modification of the shape of the island leads to a change in the dependency of the chemical potential with respect to the island height h_0 , and as a consequence this slows down the coarsening dynamics.

We first present the one dimensional dynamical model, which takes into account the

anisotropy of surface energy and is based on the resolution of the equation of continuum elasticity. Secondly, we describe analytically the equilibrium shape of one dimensional pyramidal island. From our model, we estimate the dependency of the chemical potential as a function of the island height. Thirdly, we use the relations obtained in the previous part to propose a simple dynamical model in order to explain how the coarsening time of two anisotropic strained islands increases as a function of the anisotropy strength. We conclude our article by illustrating our results with the numerical simulations of the coarsening of an array of islands in the presence of anisotropy.

II. CONTINUUM MODEL

Semiconductors film dynamics can be modelled by a mass conservation equation which takes into account the surface diffusion. This surface diffusion current is proportional to gradients of the surface chemical potential μ . In the absence of evaporation the 1D equation for the top surface of the film $h(x, t)$ reads:

$$\frac{\partial h}{\partial t} = \mathcal{D} \sqrt{1 + h_x^2} \frac{\partial^2 \mu}{\partial s^2}, \quad (1)$$

where \mathcal{D} is the diffusion coefficient, h_x is the slope of the surface height $\partial_x h(x, t)$ and $\partial/\partial s$ the surface gradient [31, 32].

The chemical potential μ at the surface is defined by:

$$\mu = \delta \mathcal{F} / \delta h. \quad (2)$$

Here \mathcal{F} is the free energy of the system which encompasses the surface and the elastic contribution $\mathcal{F} = \mathcal{F}_s + \mathcal{F}_{el}$ and $\mu = \mu_s + \mu_{el}$. The surface energy reads

$$\mathcal{F}_s = \int \gamma(h, h_x) \sqrt{1 + |h_x|^2} dx. \quad (3)$$

It includes both wetting effects and surface energy anisotropy. The elastic energy is given by the integration over both the film and the substrate of the elastic energy density, it reads:

$$\mathcal{F}_{el} = \int_{z < h(x)} \mathcal{E}_{el}(x, z) dx dz. \quad (4)$$

The elastic energy density \mathcal{E}_{el} can be computed using the values of the stress tensor σ_{ij} and of the strain tensors e_{ij} . It reads,

$$\mathcal{E}_{el} = \frac{1}{2} \sigma_{ij} e_{ij}. \quad (5)$$

As a first approximation, we examine a decomposition of the surface energy $\gamma(h, h_x)$ where the wetting and anisotropic effect are independent:

$$\gamma(h, h_x) = \gamma_f [\gamma_h(h) + \gamma_a(h_x)]. \quad (6)$$

The wetting effects are linked to the film thickness h through $\gamma_h(h) = c_w \exp(-h/\delta_w)$, where c_w and δ_w are respectively the amplitude and the range of the wetting potential [33]. We choose the anisotropy term in the surface energy to have a single minimum at a value $\tan(\theta) = \tan(\theta_e)$, as shown in Fig. 1:

$$\gamma_a(h_x) = 1 - \alpha h_x^2 \left(1 - \frac{h_x^2}{2 \tan^2(\theta_e)} \right). \quad (7)$$

Here α is the anisotropy strength and $h_x = \tan(\theta)$ is the surface slope.

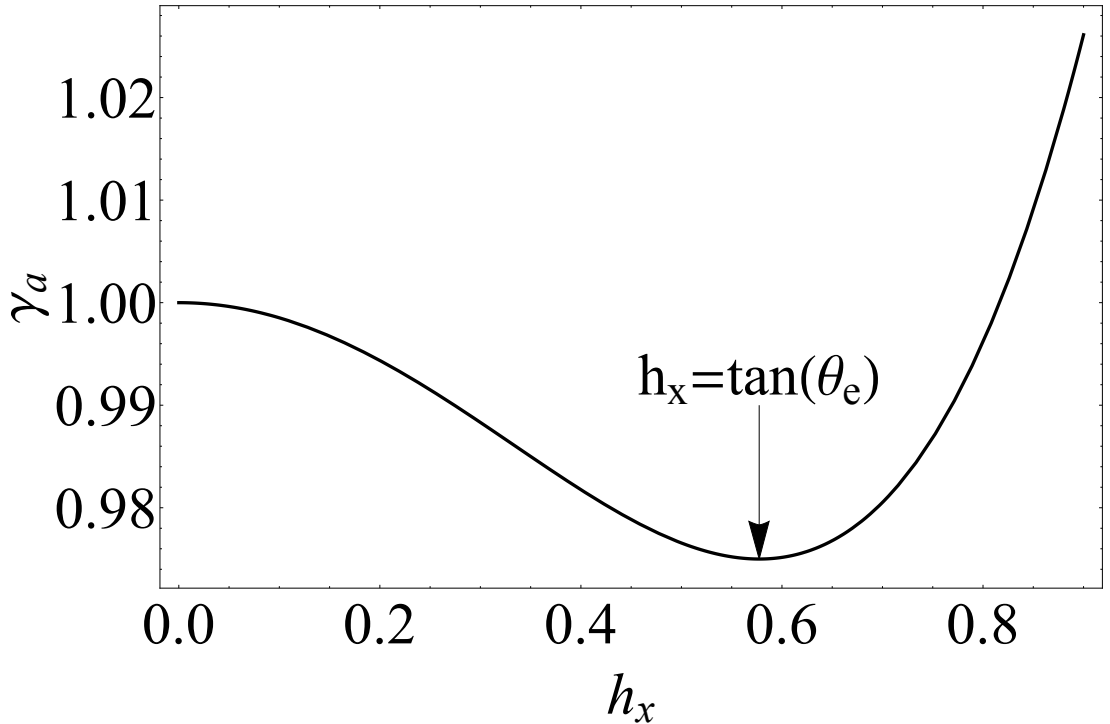


FIG. 1: Surface energy described by the anisotropy function given by Eq. (7) as a function of h_x , for $\alpha = 0.15$ and $\theta_e = \pi/6$. The minimum is given at $h_x = \tan(\theta_e)$ and represents the characteristic island slope. The vertical axis is in unit of γ_f .

Using Eq. (2) and Eq. (6), the surface chemical potential μ_s is found to be:

$$\mu_s = - \left[1 - 2\alpha + A(\alpha, \theta_e)h_x^2 + B(\alpha, \theta_e)h_x^4 \right] h_{xx} - \frac{c_w}{\delta_w} e^{-h/\delta_w}. \quad (8)$$

Here the parameters $A(\alpha, \theta_e)$ and $B(\alpha, \theta_e)$ are defined as

$$A(\alpha, \theta_e) = \frac{3}{2} \left[-1 - 4\alpha + 4\alpha \cot^2(\theta_e) \right], \quad (9)$$

$$B(\alpha, \theta_e) = \frac{15}{8} \left[1 + 2\alpha + 4\alpha \cot^2(\theta_e) \right]. \quad (10)$$

The elastic chemical potential can be written as

$$\mu_{el} = -\mathcal{H}(h_x). \quad (11)$$

where $\mathcal{H}(h_x)$ is the Hilbert transform of the spatial derivative of $h(x, t)$, defined as $\mathcal{F}^{-1}(|k|\mathcal{F}(h))$, where \mathcal{F} is the Fourier transform [34]. Thus the total chemical potential μ reads,

$$\mu = \mu_s + \mu_{el}. \quad (12)$$

The evolution equation for the surface $h(x, t)$ will merely follow from Eq. (1) and from the expression of the surface chemical potential Eq. (8) and of the elastic chemical potential Eq. (11). We first consider the space scale

$$l_0 = \gamma_f / [2(1 + \nu)\mathcal{E}_0], \quad (13)$$

resulting from the balance between the typical surface energy γ_f and the elastic energy \mathcal{E}_0 density. Here $\mathcal{E}_0 = E\eta^2/(1 - \nu)$ where $\eta = (a_f - a_s)/a_s$ is the misfit parameter where a_f (resp. a_s) is the film (resp. substrate) lattice spacing, E is the Young's modulus of the film and the substrate, and ν the Poisson's coefficient. Secondly we consider the time scale

$$t_0 = l_0^4 / (\mathcal{D}\gamma_f), \quad (14)$$

where \mathcal{D} is the surface diffusion coefficient. In units of l_0 and t_0 , the evolution equation reads

$$\frac{\partial h}{\partial t} = \frac{\partial^2 \mu}{\partial x^2} = \frac{\partial^2 (\mu_s + \mu_{el})}{\partial x^2}, \quad (15)$$

where μ_s and μ_{el} are given by Eqs. (8) and (11) respectively.

The numerical integration of Eq. (15) is performed using a pseudo-spectral method as used in [29, 34] on a periodic domain of size L_T . For example, for a $\text{Si}_{0.75}\text{Ge}_{0.25}$ film on

Si, we find $l_0 = 27$ nm and $t_0 = 23$ s at 700° C (see [35] for an estimate of surface diffusion coefficients). Eq. (15) is parametrised by the wetting constant c_w and δ_w and the anisotropy constants α and θ_e . It is a non-linear equation and its evolution is dominated by a coarsening phenomenon in which small islands disappear at the benefit of larger islands. The quantity S defined as the surface of the system

$$S = \int_{-L_T}^{L_T} h(x) dx, \quad (16)$$

is conserved during the dynamic as a simple consequence of the form of Eq. (15).

III. ANALYTICAL MODEL AND NUMERICAL SIMULATIONS

In this section, we first study the equilibrium shape of one island. Using a simple *ansatz*, we analytically determine the characteristics parameters of the island such as its size, height and energy. Our predictions are in good agreement with our numerical computation. We show that there is a smooth transition from parabolic-like to pyramid-like shapes as S increases. Secondly, we derive a dynamical model which shows that the influence of the anisotropy strength α is to increase the coarsening time. Finally, we illustrate our article with the numerical simulations of an array of islands displaying coarsening.

A. Equilibrium

The equilibrium shape of one island is given by the time independent stationary solution of Eq. (15) as shown in Fig. 2. This solution is characterised by the constant value of the chemical potential μ along the x axis. The island-like shape can be described using the following *ansatz* for the function $h(x)$:

$$h(x) = \begin{cases} h_w + \tan(\theta_e)(x + L) & -L < x < -x_1, \\ h_0 - \frac{\tan(\theta_e)}{2x_1}x^2 & -x_1 \leq x \leq x_1, \\ h_w - \tan(\theta_e)(x - L) & x_1 < x < L, \\ h_w & |x| \geq L. \end{cases} \quad (17)$$

This pyramidal-like shape describes an island of maximum height h_0 which sits on a wetting layer of height h_w . The island sides are described by straight lines of slope $\pm \tan(\theta_e)$

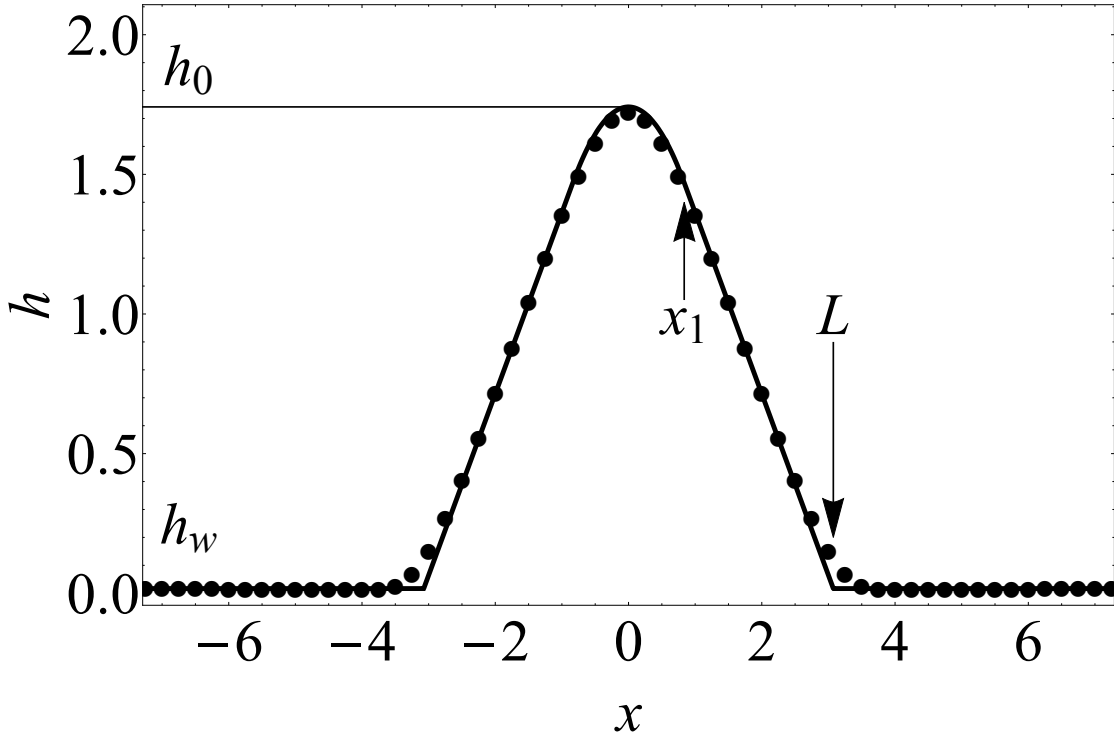


FIG. 2: Island like solution given by the numerical simulation of Eq. (15) represented by dots, compared to the *ansatz* proposed in Eq. (17) represented by the continuous curve. L is the half-width of the island and x_1 is the top island parabola width. We use as parameters $c_w = 0.045$ and $\delta = 0.005$. The initial condition is given by a small random perturbation around a constant value of $h = 0.4$. The value of the surface is $S = 6.1$. The anisotropic parameters are $\alpha = 0.1$ and $\theta_e = \pi/6$. The system size is $L_T = 16$.

for $-L < x < -x_1$ and $x_1 < x < L$. The island top is described by a parabola for $-x_1 < x < x_1$, which satisfies the continuity of the first derivative of $h(x)$ at $x = \pm x_1$. At the foot of the island $|x| = L$ the function $h(x)$ is continuous and has a value h_w . Here x_1 is the half-width of the parabola.

This *ansatz* is characterised by four unknown parameters (h_0, h_w, x_1, L) which can be deduced from four relations. The first relation is the continuity of $h(x)$ at $x = \pm x_1$, it imposes:

$$h_0 = h_w + \tan(\theta_e)(L - x_1/2). \quad (18)$$

After the substitution of the *ansatz* (17), we expand Eq. (15) around $x = 0$ in a polynomial series up to second order in x . At order 0 in x , we obtain the value of the half-width

island L

$$L = \exp\left(\frac{\pi(1 - 2\alpha) - \pi\mu x_1 \cot(\theta_e) + 2x_1(\log(x_1) - 1)}{2x_1}\right). \quad (19)$$

Here the chemical potential μ reads:

$$\mu = -\frac{c_w}{\delta_w} e^{-h_w/\delta_w}. \quad (20)$$

This previous relation is due to the fact that far from the island the film is flat, so that h_x and h_{xx} vanish, and only the wetting potential term remains dominant in Eq. (8) and (11).

The chemical potential μ being fixed, the wetting layer value h_w reads:

$$h_w = -\delta_w \log\left(\mu \frac{\delta_w}{c_w}\right). \quad (21)$$

From the expansion at second order in x of Eq.(15), we obtain a transcendental equation for x_1 , it reads:

$$\frac{\tan(\theta_e) \left(\frac{1}{L^2} + \frac{6\pi\alpha + x_1}{x_1^3}\right)}{\pi} - \frac{3(4\alpha + 1) \tan^3(\theta_e)}{2x_1^3} = 0. \quad (22)$$

Combining Eq. (19) and Eq. (22), we obtain the following transcendental equation for the parameter x_1 ,

$$\left(\frac{1}{\pi} \exp\left(-\frac{\pi(1 - 2\alpha) - \pi\mu x_1 \cot(\theta_e) + 2x_1(\log(x_1) - 1)}{x_1}\right) + \frac{6\alpha}{x_1^3} + \frac{1}{\pi x_1^2}\right) - \frac{3(4\alpha + 1) \tan^2(\theta_e)}{2x_1^3} = 0. \quad (23)$$

After substitution of Eq. (20) in Eq. (23), we can solve Eq. (23) numerically using a simple root finding algorithm to obtain the parameter x_1 for different values of h_w . The island half-width L can then be deduced from Eq. (19). Furthermore the value of the island height h_0 can be deduced from Eq. (18). For each value of the wetting layer height h_w , we can compute the value of the surface S (mass) using Eq. (16) and the *ansatz* Eq. (17). Finally, from the knowledge of the values (h_0, L, x_1, μ) , we can compute the value of the surface S , it reads:

$$S = 2[h_0 x_1 + h_w(L_T - x_1)] + (3L^2 - 6Lx_1 + 2x_1^2) \frac{\tan(\theta_e)}{3}. \quad (24)$$

We present in Fig. 2 the island shape numerically integrated from Eq. (15) and compare it with the *ansatz* (17). The agreement is quite satisfactory and there are no free parameters.

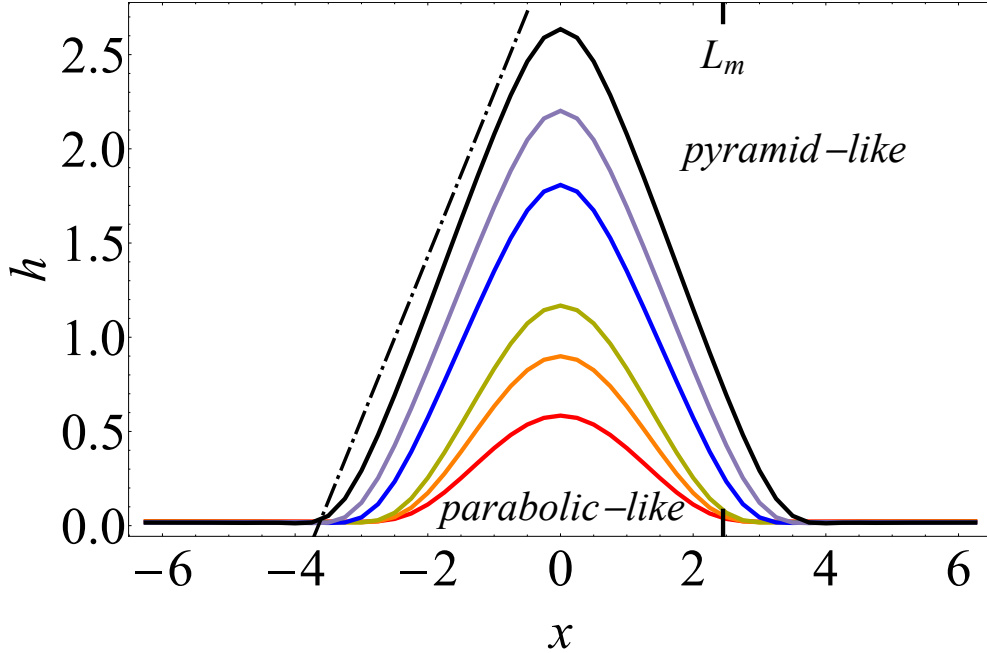


FIG. 3: Numerical island profile computed from Eq. (15) for different initial values of the surface S . For small surface S , we obtain a parabolic-shaped island, with constant island width. For island surfaces larger than $S_m = 3.7$, the islands present a pyramidal-like shape. Its characteristic half-width $L_m = 2.26$, given by Eq. (25), is represented in the figure. From bottom to top: Red-Curve bottom ($S = 1.80$), Orange ($S = 2.66$), Green ($S = 3.48$), Blue ($S = 5.84$), Purple ($S = 7.58$), Black ($S = 9.74$), color on-line. The dashed-dotted curve represent the characteristic slope given by $\tan(\theta_e)$, in this case $\theta_e = \arctan(\sqrt{3/4})$.

When the horizontal size of the parabola $2x_1$ becomes smaller than the island size L , the island morphology changes from pyramid-like shape to a parabolic-like shape. Using Eq. (19) and Eq. (24) we obtain

$$L_m = \frac{3}{5}\pi \sec^2(\theta_e)(1 - (8\alpha + 1) \cos(2\theta_e)), \quad (25)$$

$$S_m = \frac{2}{3}L_m [3(h_0 + h_w) + L_m \tan(\theta)]. \quad (26)$$

Therefore, the pyramidal shape can only exist for $S > S_m$ and $L > L_m$. Below this value of S_m , the islands are parabolic-like shaped and the anisotropy can be neglected.

We plot in Fig. 3 various island profiles obtained by numerical simulation for different initial values of the surface S . Our numerical simulation shows that for a small island surface

S , the island shape is parabolic-like and its widths L is rather constant. As the surface of the system increases the islands become pyramid-like and their widths increase smoothly with respect to their height. The transition from parabolic-like shape to pyramid is smooth as the control parameter S is varied.

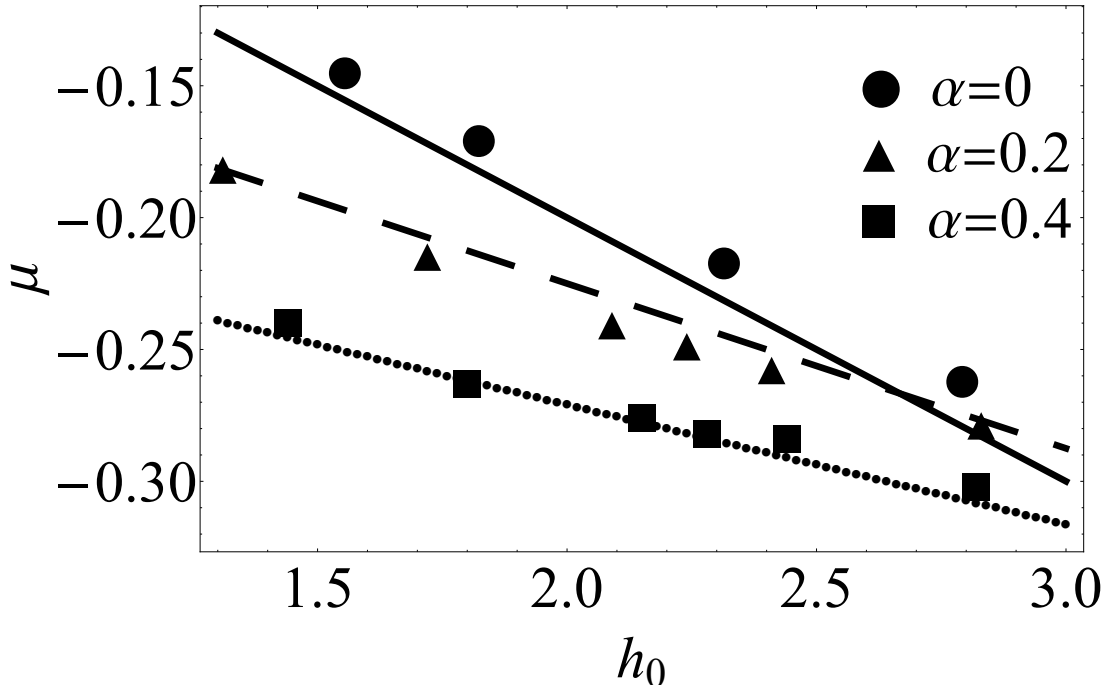


FIG. 4: Chemical potential μ as a function of the island height h_0 at equilibrium with $\theta_e = \pi/6$. The \bullet , \blacktriangle and \blacksquare symbols are computed by numerical integration of Eq. (15) for $\alpha = 0$, $\alpha = 0.2$ and $\alpha = 0.4$ respectively. The continuous, dashed and dotted curves represent the solution given by Eq. (27) for $\alpha = 0$, $\alpha = 0.2$ and $\alpha = 0.4$ respectively. The approximation given by Eq. (27) fits the results of the numerical solution.

Finally, we compute the value of the chemical potential as a function of the island height for various value of the anisotropy strength α . As shown in Fig. 4, the chemical potential decays quasi-linearly as a function of the island height as shown below in Eq. (27).

Using Eq. (23) the chemical potential μ can be expressed easily as a function of the parameter x_1 . In the same way using Eq. (18) the island height can be expressed as a function of x_1 . Finally using the relation $\frac{\partial \mu}{\partial h} = \frac{\partial \mu}{\partial x_1} \frac{\partial x_1}{\partial h}$ the slope of the chemical potential versus the height of the island for small values of α is found to be:

$$\frac{\partial \mu}{\partial h} \simeq -\frac{1}{1 + 3\alpha}. \quad (27)$$

B. Dynamics

1. Numerical simulation of the coarsening of two islands and dynamical model

In this subsection, we characterise the dynamic of coarsening of two islands. In Fig. 5, we show the time evolution of two pyramidal-shaped islands obtained by the numerical simulation of Eq. (15). During the coarsening, the larger island increases at expense of the smaller island until it disappears. Ultimately at a time t_c defined as the coarsening time only one island remains in the system. The initial conditions are prepared following [32], by replicating a pyramid with a slight difference in amplitude. In order to analyse this

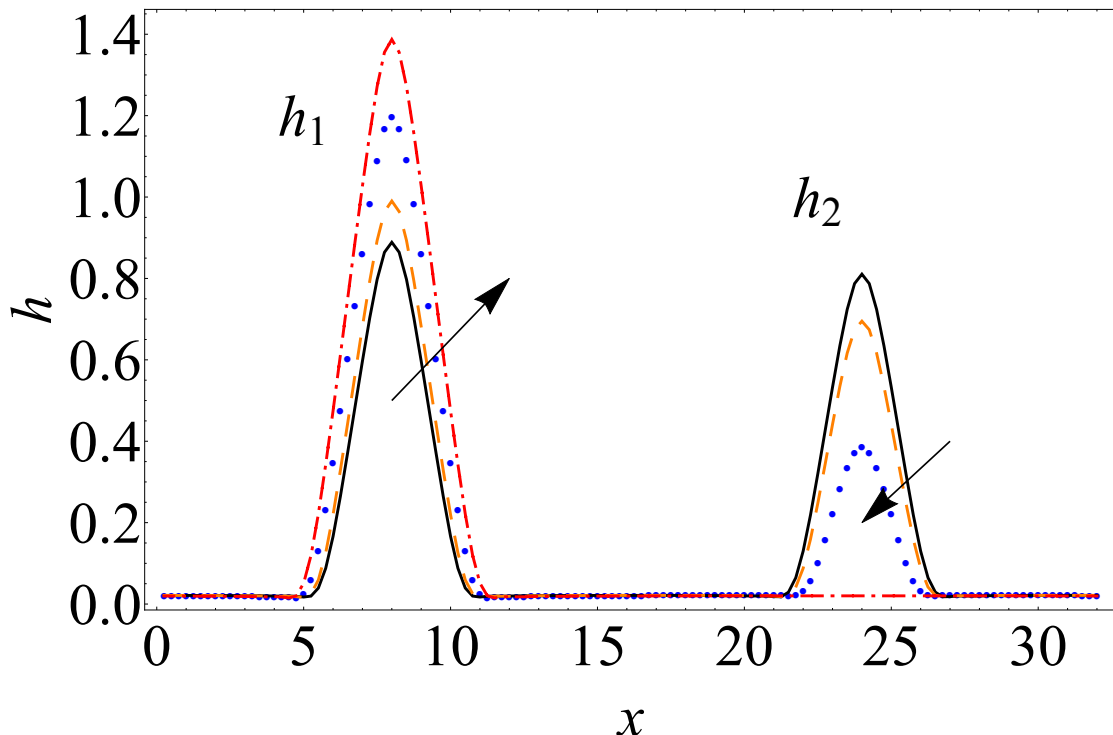


FIG. 5: Spatio temporal evolution of two islands, deduced by numerical simulation of Eq. (15). The initial condition are two islands of height $h_1(0) = 0.89$ and $h_2(0) = 0.8$ separated a distance $d = L_T/2$, where $L_T = 32$ represents the system size. The anisotropic parameters are $\alpha = 0.1$ and $\theta = \pi/6$. The continuous curve (black) represents the island profile at $t = 1$, dashed curve (orange) $t = 30$, dotted curve (blue) $t = 80$ and dotted-dashed curve (red) $t = 100$. After a time $t_c = 88$, there remains only one island in the system.

phenomenon, we propose a simple model for the coarsening of two islands, inspired by the

work presented in [32]:

$$\begin{aligned} h_1 \partial_t h_1 &= \tan(\theta_e) \frac{\mu(h_2) - \mu(h_1)}{d}, \\ h_2 \partial_t h_2 &= \tan(\theta_e) \frac{\mu(h_1) - \mu(h_2)}{d}. \end{aligned} \quad (28)$$

Here $h_1(t)$ is the height of the large island, $h_2(t)$ is the height of the small one and d is the distance separating them. If we consider the island width as $h_i / \tan(\theta_e)$, we recover the model proposed in [32]. The advantage of this model is that its resolution requires only the resolution of a differential equation instead of the resolution of a partial differential equation.

In Fig. 6, we represent the time evolution of each islands heights h_1 and h_2 , corresponding to the result displayed in Fig. 5. We also compare in Fig. 6 the results obtained from the resolution of the model Eq. (28) with results of the numerical simulation of Eq. (15). The model predictions is in good agreement with the numerical simulation of Eq. (15). The resolution of the model can be done in two ways: a simple numerical integration of Eq. (28) or an analytical resolution of Eq. (28) as explain in section III.B.2. The slight discrepancy between the numerical result (numerical simulation of Eq. (15)) and theoretical result (resolution of the puntual model Eq. (28)) for the final height h_1 is mostly due to the fact that our model is based on a simple pyramidal-like shape *ansatz* during all the coarsening dynamic. This small discrepancy in the height does not affect the coarsening time t_c .

2. Effect of the anisotropy on the coarsening time

In Fig. 7, we present the coarsening time t_c of two strained islands as a function of the anisotropy strength α . We compare the analytical coarsening time t_c obtained by the resolution of the model Eq. (33) and the results obtained by numerical simulation of Eq. (15). There is a good agreement between both results. As shown in Fig. 7 we find that the coarsening time increase linearly as a function of the anisotropy strength α . We can explain this effect in the following way.

Using Eq. (28) it can be easily shown that $\partial_t(h_1^2 + h_2^2) = 0$. We thus propose the following change of variables in order to solve analytically Eq. (28):

$$\begin{aligned} h_1(t) &= h_0 \sin(\phi(t)), \\ h_2(t) &= h_0 \cos(\phi(t)). \end{aligned} \quad (29)$$

Here h_0 is related to the initial islands heights as $h_0 = \sqrt{h_1(0)^2 + h_2(0)^2}$. Substituting Eq. (29) into Eq. (28) yields:

$$\partial_t \phi = \frac{\tan(\theta_e)}{h_0 d (1 + 3\alpha)} \left(\frac{1}{\cos(\phi)} - \frac{1}{\sin(\phi)} \right), \quad (30)$$

submitted to the initial condition $\phi(0) = \phi_0 = \arctan\left(\frac{h_1(0)}{h_2(0)}\right)$. Eq. (30) can be integrated analytically, its solution is

$$t(\phi) = (1 + 3\alpha)d \frac{h_0}{\tan(\theta_e)} \mathcal{T}(\phi). \quad (31)$$

The analytical form of $\mathcal{T}(\phi)$ is given in [36]. The coarsening time t_c is defined by the following criteria: when the height of the small island reaches the wetting layer height h_w . This implies the following implicit relation for t_c :

$$\phi(t_c) = \arcsin\left(\frac{h_w}{h_0}\right). \quad (32)$$

This previous relation derives from Eq. (29) easily. Using Eq. (31) we obtain the coarsening time t_c . It reads:

$$t_c = (1 + 3\alpha)d \frac{h_0}{\tan(\theta_e)} \mathcal{T}[\phi(t_c)], \quad (33)$$

this result agrees with the numerical simulation presented in Fig. 7. In the limit of $(h_w/h_0) \ll 1$, the expression $\mathcal{T}(\phi(t_c))$ can be simplified as given in [37].

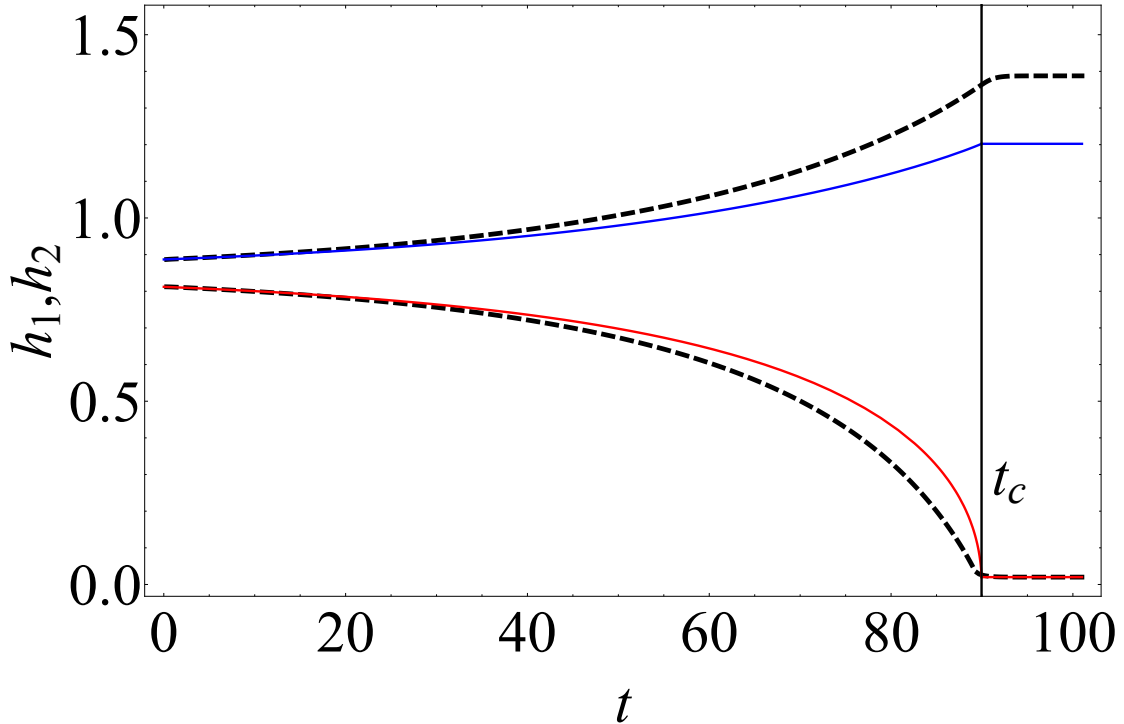


FIG. 6: Time evolution of the height h_1 and h_2 , corresponding to the result shown in Fig. 5. The dashed curves represent the islands heights given by the numerical simulation of Eq. (15), and the continuous curves represent the result obtain by the numerical resolution of the dynamical model presented in Eq. (28). The same results for the continuous curve can be obtained analytical as explained in section III.B.2. The coarsening time is $t_c = 88$ for both solutions. The vertical axes is in units of l_0 and the time scale is t_0 .

3. Numerical simulation of an array of islands with anisotropy

For illustration, we present the numerical simulation of the coarsening of an array of islands. The numerical simulation of Eq. (15) reveals mostly two phenomena. A first instability regime which arises for an initial film height higher than the critical layer. A second regime in which coarsening takes place and is not interrupted. As shown in Fig. 8 after the initial instability the smaller islands vanish by surface diffusion through the wetting layer at the benefit of the bigger islands until the system reach the equilibrium. The equilibrium state is characterised by a large island whose characteristic size can be deduced from the parameters of the Eq.(17). This phenomenon is observed numerically with or

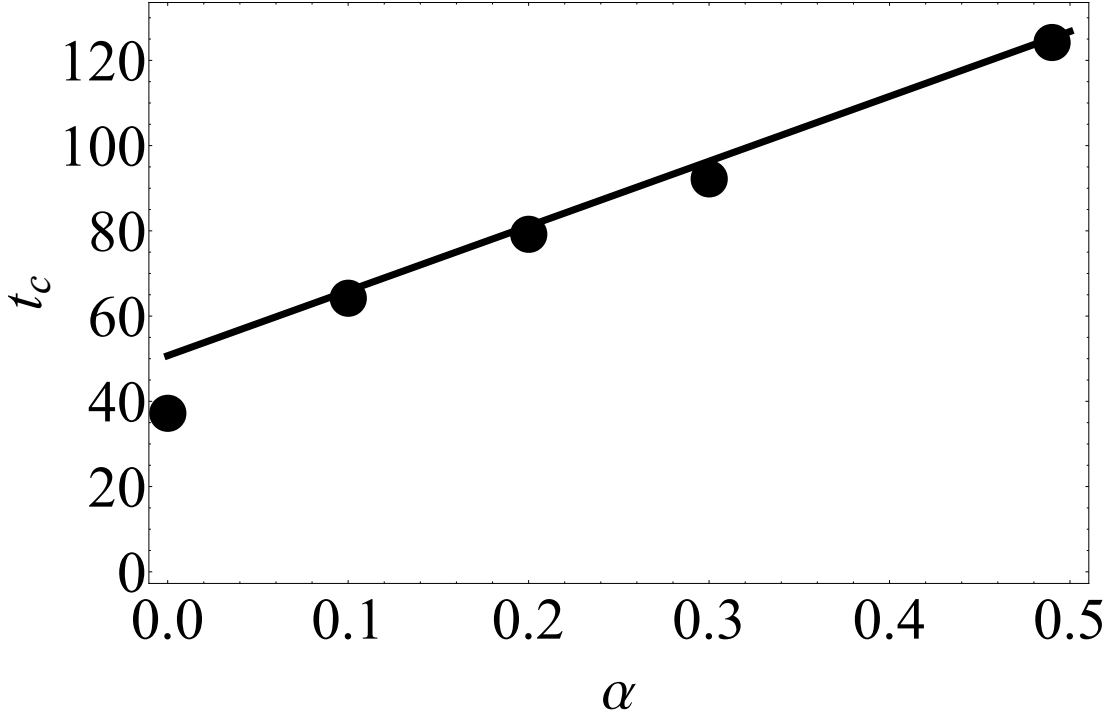


FIG. 7: Coarsening time t_c as a function of the anisotropy strength α . The system under study is the same as shown in Fig. 5. The dots represents the numerical simulation of Eq. (15) and the curve is the solution for t_c given by Eq. (33). The coarsening time t_c depends linearly on α .

without the presence of the surface energy anisotropy.

We show in Fig. 9 an ensemble average for the maximum height of h as a function of time computed by numerically integrating Eq. (15). The results are presented for three different values of the anisotropy strength ($\alpha = 0$, $\alpha = 0.01$ and $\alpha = 0.05$). We have performed twenty numerical simulation for each value of α . We observe that the rate coarsening of an anisotropic system ($\alpha = 0.01$ and $\alpha = 0.05$) is slower than the system without anisotropy ($\alpha = 0$). This effect is due to the increase of the coarsening time t_c as described previously in Fig. 7. Finally, we note that the determination of the coarsening exponent reported in [34] is still under investigation in presence or absence of surface anisotropy. As matter of fact the understanding of the dynamics between the islands could serve to elaborate an analytical model to describe the coarsening dynamic of a many islands system.

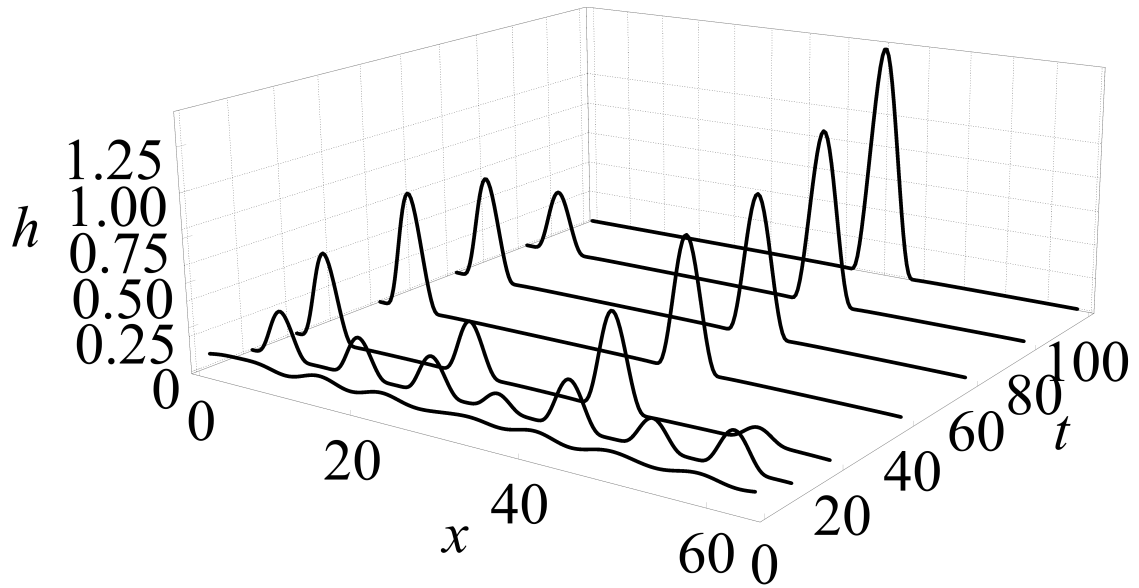


FIG. 8: Evolution of an anisotropic strained islands according to Eq. (15), where the initial condition is a flat film of height 0.11 with a small random perturbation. First the ATG instability evolves, and the coarsening start after the islands have formed. Finally, there is only one pyramidal-shape island with the characteristic slope shown in Fig. 1.

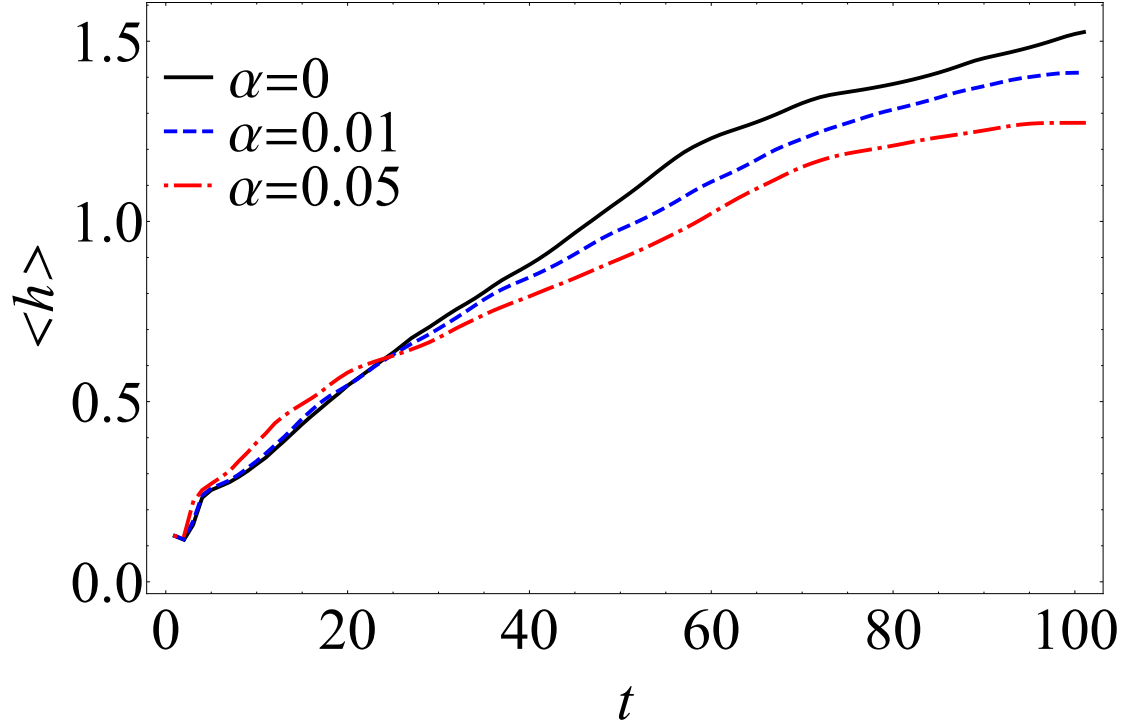


FIG. 9: Ensemble average for the maximum height h as a function of time for three different values of α . $\alpha = 0$ (continuous line), $\alpha = 0.01$ (dashed line) represented in Fig. 8 and $\alpha = 0.05$ (dashed-dotted line) obtain by the numerical simulation of Eq. (15). The initial condition for the systems is a flat film of height 0.1 with a small random perturbation. The maximum value of h is calculated using an ensemble average of twenty simulations for each different α .

IV. CONCLUSION

This article presents a numerical and analytical study of the shape and of the dynamics coarsening of strained anisotropic islands. We have characterised analytically strained islands using a simple *ansatz*. We have introduced a dynamical model to investigate the dynamics of coarsening of two islands. This model compares favorably with our numerical simulation. We have shown that the coarsening dynamics of strained island in hetero-epitaxy is slowed down by the presence of the surface energy anisotropy. Our results are in good agreement with our numerical simulations. For future work the comparison to experiments will be investigated in three dimensions.

Acknowledgments

We would like to thank Franck Celestini, Jean-Noël Aqua, Pierre Müller and Julien Brault for useful discussions. We thank the ANR NanoGaNUV for financial support.

-
- [1] A. Pimpinelli and J. Villain, *Physics of Crystal Growth*, Collection Alea-Saclay: Monographs and Texts in Statistical Physics (Cambridge University Press, 1998).
 - [2] P. Politi, G. Grenet, A. Marty, A. Ponchet, and J. Villain, *Physics Reports* **324**, 271 (2000).
 - [3] J. E. Ayers, *Heteroepitaxy of Semiconductors: Theory, Growth, and Characterization* (CRC Press, 2007).
 - [4] V. A. Shchukin and D. Bimberg, *Rev. Mod. Phys.* **71**, 1125 (1999).
 - [5] J. Stangl, V. Holý, and G. Bauer, *Rev. Mod. Phys.* **76**, 725 (2004).
 - [6] J. Brault, S. Matta, T.-H. Ngo, D. Rosales, M. Leroux, B. Damilano, M. A. Khalfioui, F. Tendille, S. Chenot, P. D. Mierry, et al., *Materials Science in Semiconductor Processing* **55**, 95 (2016).
 - [7] B. J. Spencer, P. W. Voorhees, and S. H. Davis, *Phys. Rev. Lett.* **67**, 3696 (1991).
 - [8] P. Müller and A. Saúl, *Surface Science Reports* **54**, 157 (2004).
 - [9] C.-H. Chiu and Z. Huang, *Applied Physics Letters* **89**, 171904 (2006).
 - [10] J.-N. Aqua, A. Gouyé, A. Ronda, T. Frisch, and I. Berbezier, *Phys. Rev. Lett.* **110**, 096101 (2013).

- [11] J.-N. Aqua, I. Berbezier, L. Favre, T. Frisch, and A. Ronda, *Physics Reports* **522**, 59 (2013), growth and self-organization of SiGe nanostructures.
- [12] B. J. Spencer and J. Tersoff, *Phys. Rev. B* **87**, 161301 (2013).
- [13] C. Wei and B. J. Spencer, *Proceedings. Mathematical, Physical, and Engineering Sciences* **472**, 2190 (2016).
- [14] F. Rovaris, R. Bergamaschini, and F. Montalenti, *Phys. Rev. B* **94**, 205304 (2016).
- [15] C. Wei and B. J. Spencer (2017), arXiv:1704.03457.
- [16] D. Srolovitz, *Acta Metallurgica* **37**, 621 (1989).
- [17] Y.-W. Mo, D. E. Savage, B. S. Swartzentruber, and M. G. Lagally, *Phys. Rev. Lett.* **65**, 1020 (1990).
- [18] D. J. Eaglesham and M. Cerullo, *Phys. Rev. Lett.* **64**, 1943 (1990).
- [19] J. A. Floro, E. Chason, L. B. Freund, R. D. Twisten, R. Q. Hwang, and G. A. Lucadamo, *Phys. Rev. B* **59**, 1990 (1999).
- [20] P. Sutter and M. G. Lagally, *Phys. Rev. Lett.* **84**, 4637 (2000).
- [21] R. M. Tromp, F. M. Ross, and M. C. Reuter, *Phys. Rev. Lett.* **84**, 4641 (2000).
- [22] J. A. Floro, M. B. Sinclair, E. Chason, L. B. Freund, R. D. Twisten, R. Q. Hwang, and G. A. Lucadamo, *Phys. Rev. Lett.* **84**, 701 (2000).
- [23] I. Berbezier and A. Ronda, *Surface Science Reports* **64**, 47 (2009).
- [24] C. Misbah, O. Pierre-Louis, and Y. Saito, *Rev. Mod. Phys.* **82**, 981 (2010).
- [25] R. J. Asaro and W. A. Tiller, *Metallurgical Transactions* **3**, 1789 (1972).
- [26] M. A. Grinfeld, *Sov. Phys. Dokl.* **31**, 831 (1986).
- [27] J. Tersoff, B. J. Spencer, A. Rastelli, and H. von Känel, *Phys. Rev. Lett.* **89**, 196104 (2002).
- [28] Y. W. Zhang, *Phys. Rev. B* **61**, 10388 (2000).
- [29] J.-N. Aqua and T. Frisch, *Phys. Rev. B* **82**, 085322 (2010).
- [30] M. Korzec and P. Evans, *Physica D: Nonlinear Phenomena* **239**, 465 (2010).
- [31] M. S. Levine, A. A. Golovin, S. H. Davis, and P. W. Voorhees, *Phys. Rev. B* **75**, 205312 (2007).
- [32] G. Schifani, T. Frisch, M. Argentina, and J.-N. Aqua, *Phys. Rev. E* **94**, 042808 (2016).
- [33] P. Müller and R. Kern, *Applied Surface Science* **102**, 6 (1996).
- [34] J.-N. Aqua, T. Frisch, and A. Verga, *Phys. Rev. B* **76**, 165319 (2007).
- [35] J. A. Floro, E. Chason, L. B. Freund, R. D. Twisten, R. Q. Hwang, and G. A. Lucadamo,

Phys. Rev. B **59**, 1990 (1999).

[36] $\mathcal{T}(\phi) = (\sin(\phi) - \sin(\phi_0) + \cos(\phi) - \cos(\phi_0) - \sqrt{2} \tanh^{-1} \left[\frac{1}{\sqrt{2}} \left(\tan \left(\frac{\phi}{2} \right) + 1 \right) \right] + \sqrt{2} \tanh^{-1} \left[\frac{1}{\sqrt{2}} \left(\tan \left(\frac{\phi_0}{2} \right) + 1 \right) \right])$ where $h_0 = \sqrt{h_1(0)^2 + h_2(0)^2}$ and $\phi_0 = \phi(0) = \arctan \left(\frac{h_1(0)}{h_2(0)} \right)$

[37] $\mathcal{T}(\phi(t_c)) \simeq -\frac{h_1}{h_2 \sqrt{\frac{h_1^2}{h_2^2} + 1}} - \frac{1}{\sqrt{\frac{h_1^2}{h_2^2} + 1}} + \sqrt{2} \tanh^{-1} \left(\frac{\tan(\frac{1}{2} \tan^{-1}(\frac{h_1}{h_2})) + 1}{\sqrt{2}} \right) + 1 - \sqrt{2} \tanh^{-1} \left(\frac{1}{\sqrt{2}} \right)$. This result is obtained assuming that the wetting layer height is smaller than the initial islands heights ($h_w/h_0 \ll 1$). With this approximation $\phi(t_c) \simeq 0$.